

THE LOW MASS X-RAY BINARY-GLOBULAR CLUSTER CONNECTION II: NGC 4472 X-RAY SOURCE PROPERTIES AND SOURCE CATALOGS ¹

THOMAS J. MACCARONE², ARUNAV KUNDU³ AND STEPHEN E. ZEPF³
Draft version March 8, 2019

ABSTRACT

We present the results of a Chandra/HST study of the point sources of the Virgo cluster giant elliptical galaxy NGC 4472. We identify 144 X-ray point sources outside the nuclear region, 72 of which are located within the HST fields. The optical data show 1102 sources, of which 829 have colors consistent with being globular clusters (with only 4 in the restricted central 10" region). Thirty matches are found between the two lists - these are likely to be low mass X-ray binaries associated with globular clusters, while forty-two of the X-ray sources have no optical counterparts to $V \lesssim 25$ and $I \lesssim 24$, indicating that they are likely to be predominantly low mass X-ray binaries in the field star population with a small amount of possible contamination from background active galactic nuclei. Thus approximately 40% of the X-ray sources are in globular clusters and $\sim 4\%$ of the globular clusters contain X-ray sources. There is suggestive evidence that the X-ray sources located in blue globular clusters may have harder X-ray spectra than those located in red globular clusters. No statistically significant differences are found between the X-ray properties of the field sources and the X-ray properties of the sources located in globular clusters. This study, along with our previous result from Paper I in this series on the similarity of the spatial profile of the field LMXBs, globular cluster LMXBs, and the globular clusters themselves suggest that a significant fraction of the observed low mass X-ray binaries in the field may be created in a globular cluster then ejected into the field by stellar interactions; however, by comparing the results for NGC 4472 with those in several other galaxies, we find tentative evidence for a correlation between the globular cluster specific frequency and the fraction of LMXBs in globular clusters, a correlation which would be most easily explained if some of the field sources were generated *in situ*. We show that isolated accreting very massive black holes are unlikely to be observable with current X-ray instrumentation and that these sources hence do not contaminate the LMXB population. We discuss the possibility that several equatorial point sources may indicate the presence of a disk wind responsible for the low radiative efficiency observed in the nucleus of this source.

Subject headings: galaxies:general – galaxies:individual(NGC 4472) – galaxies:star clusters – globular clusters:general – X-rays:binaries – X-rays:galaxies

1. INTRODUCTION

Early X-ray studies of elliptical and S0 galaxies showed that they were significant sources of X-ray emission, with both a soft, $kT \sim 1$ keV X-ray component and a harder X-ray component (fitting to a ~ 6 keV bremsstrahlung spectrum or a $\frac{dN}{dE} \propto E^{-1.7}$ power law) with a flux roughly proportional to the optical luminosity (White, Sarazin & Kulkarni 2002 and references within). The soft component is associated with hot virialized interstellar gas while the hard component is associated with low mass X-ray binaries - systems where a neutron star or black hole is accreting gas from a Roche lobe overflowing companion star (e.g. Forman, Jones & Tucker 1985; Trinchieri & Fabbiano 1985). Since the advent of the Chandra X-ray Observatory, these X-ray binaries have been resolved, with about half typically associated with globular clusters, ranging from at least 70% in NGC 1399 (Angelini, Loewenstein & Mushtozky 2001) to 40% in NGC 4472 (Kundu, Maccarone & Zepf 2002 - hereinafter Paper I), and a lower limit of 20% in NGC 4697 (Sarazin, Irwin & Bregman 2000).

The lifetime of an X-ray source steadily accreting at the typical 10^{37} ergs/second detection threshold for Chandra observations of elliptical galaxy is no more than a few hundred million years (see e.g. Bhattacharya 1995). Thus for a low mass X-ray binary (LMXB) in an elliptical galaxy to be observable with Chandra, it must either have been recently formed or it must be an outbursting transient system (Piro & Bildsten 2002). Most of the low mass X-ray binaries in spiral galaxies are formed when a massive star in a tight binary system undergoes a supernova explosion and leaves behind a compact remnant in a close enough orbit for Roche lobe overflow from the secondary star to occur. In most elliptical galaxies, little or no star formation has occurred for several billion years, so the only means of LMXB formation are stellar interactions or the evolution off the main sequence of a binary companion to a compact star. In contrast to low mass X-ray binaries, high mass X-ray binaries are those systems where the accretion is driven by the compact object's capture of stellar wind from a massive, secondary star (typically an O star or an early B-type star). Because the lifetimes of these early-

¹ Based on observations made with the NASA/ESA Hubble Space Telescope, obtained at the Space Telescope Science Institute, which is operated by the Association of University for Research in Astronomy, Inc., under NASA contract NAS 5-26555, and on observations made with the Chandra X-ray Observatory.

² Astrophysics Sector, SISSA/ISAS, via Beirut 4, 34014 Trieste, Italy; email: maccarone@ap.sissa.it

³ Department of Physics and Astronomy, Michigan State University, East Lansing MI, 48824; email: akundu, zepf@pa.msu.edu

type stars are typically $\sim 10^7$ years or less, high mass X-ray binaries should only appear in regions with active star formation, thus eliminating them as possible sources in low redshift elliptical galaxies and old globular clusters (i.e. all globular clusters except the very young ones seen in currently merging galaxies).

Globular clusters have long been known to be fertile breeding grounds for X-ray binaries. About 10% of the Milky Way's LMXBs are contained within globular clusters (see e.g. Liu, van Paradijs & van den Heuvel 2001 and references within), despite the fact that less than 1% of the stellar mass of the Galaxy is contained in globular clusters. The dominant mechanism for forming new X-ray binaries outside of globular clusters in spiral galaxies cannot work in elliptical galaxies. Furthermore, elliptical galaxies have higher fractions of their stellar mass in their globular clusters (see e.g. Ashman & Zepf 1998; Rhode & Zepf 2001). Hence it is not surprising that the well-observed elliptical galaxies all show much higher fractions of their LMXBs in globular clusters than does the Milky Way.

In paper I of this series, we explored what properties make a globular cluster most likely to contain an X-ray source. The red (i.e. metal rich) globular clusters are ~ 3 times as likely as the blue (i.e. metal poor) clusters to host an X-ray source. As an aside, we note that elliptical galaxies have a larger fraction of their globular cluster system in the red globular clusters, which may be an additional reason for them to have a higher fraction of their low mass X-ray binaries in globular clusters. The luminosity function for the X-ray sources associated with globular clusters is consistent with being the same as the luminosity function for the sources where there is no globular cluster counterpart. Here we extend that work by presenting the source lists of the globular clusters and the X-ray sources, and show the associated optical parameters for each X-ray source. We discuss additional possible correlations between the source parameters in greater detail than in Paper I. We compare summed X-ray spectra of field sources with globular cluster sources, of sources in blue clusters with those in red clusters, and of sources at different luminosities. We show that very massive black holes accreting from the interstellar medium cannot make up the X-ray sources in NGC 4472 or most other elliptical galaxies. We note the similarities between the properties of the field and cluster LMXBs and consider the relative merits of different scenarios for producing the field LMXB populations. We discuss the nuclear emission and the possible existence of an equatorial outflow.

2. REDUCTION PROCEDURE

2.1. X-ray Data Reduction

NGC 4472 is a giant elliptical galaxy, located at a distance of about 16 Mpc (e.g. Macri et al. 1999) in the Virgo cluster. Chandra observed NGC 4472 for 39588 seconds on June 12, 2000. We examine only the data from the ACIS-S3 detector. We remove hot columns following the guidelines on the ‘‘ACIS Recipes: Clean the Data’’ web page at Penn State University (<http://www.astro.psu.edu/xray/acis/recipes/clean.html>). Because of the large diffuse background in these observations (due to the X-ray emission from the interstellar gas)

no sources are detected with fewer than 10 counts so the flaring pixels are likely to be of minimal importance, but we nonetheless remove flaring pixels using the Flagflare script written by T. Miyaji.

We create three images for source detection - a full band image from 0.5 to 8.0 keV, a soft band image from 0.5 to 2.0 keV, and a hard band image from 2.0 to 8.0 keV. While some source photons may be missed in the 8.0-10.0 keV range, it has generally been found that this band contributed far more noise than signal even in the ACIS-I detector (see e.g. Baganoff 1999); the ACIS-S chips are more sensitive to soft X-rays than the ACIS-I, and less sensitive to hard X-rays, so ignoring the 8-10 keV band should be even more beneficial for these observations. We then run WAVDETECT from the CIAO 2.2 package using wavelet scales from 1 to 16 pixels spaced by factors of 2. We set a false source probability detection threshold of 10^{-6} , which should yield an expectation value of slightly less than one false source over the entire ACIS-S chip.

We extract spectra using the psextract script from the Chandra X-ray Center. We define the source regions to be the 3σ ellipses given by WAVDETECT and the background regions to be an elliptical annulus centered on the source position with the outer major and minor axes equal to twice the major and minor axes of the source region, respectively, and the inner region defined by the outer boundaries of the source region. The spectra are binned so that at least 20 photons from the source region (which includes some background photons) are in each channel to allow reliable χ^2 fitting, although the highest and lowest energy bins may have less than 20 photons.

We then fit the spectra in XSPEC 11.0 (Arnaud 1996) to find the fluxes. In all cases, we freeze the neutral hydrogen column to the value 1.6×10^{20} (the Galactic value from the FTOOL nH which uses the measurements of Dickey & Lockman 1990). We include channels from 0.5 to 8.0 keV and fit absorbed power law spectra for all the sources. Where there are fewer than 4 channels from 0.5-8.0 keV for the spectral fit, we freeze the spectral index, Γ (defined such that $\frac{dN}{dE} = E^{-\Gamma}$) to 2.0 and fit only the normalization. In all but a few cases, the fits give $\chi^2/\nu < 2.0$, which generally represents an acceptable fit for such a small number of photon bins. The poorly fitting sources are flagged in the table, as XSPEC will not fit error bars when $\chi^2/\nu > 2.0$. We estimate the fluxes of the sources using the flux command in XSPEC. Because the neutral hydrogen absorption is folded into the model, the fluxes for the 0.5-2.0 keV band are typically underestimated by about 5%. We then compute the inferred (0.5-8.0) keV luminosity assuming a distance of 16 Mpc (Macri et al. 1999).

2.2. Optical Data Reduction and Astrometry

Given the high density of GCs, subarcsecond relative astrometry between the Chandra and HST images is essential to accurately determine GC-LMXB overlaps and to eliminate false matches. The problem is compounded by the fact that the absolute astrometry of the Chandra image and each of the HST-WFPC2 frames may be inaccurate by $1-2''$, and very few Chandra sources are seen in the outer HST fields. We adopted the following procedure to bootstrap all the images to the USNO A2.0 (Monet et al. 1998) system: Using the IRAF TFINDER routine and

the positions of USNO A2.0 stars we first tied the large field of view, ground-based image of NGC 4472 of Rhode & Zepf (2001) to the USNO A2.0 astrometric system. We then used the positions of the globular cluster candidates identified by Rhode & Zepf (now in the USNO 2.0 system) to obtain new astrometric plate solutions for each of the four HST frames using TFINDER. The r.m.s. error of the astrometric solution achieved for each HST image, and the relative astrometry of the 4 WFPC2 frames is of the order of a hundredth of an arcsecond. In order to bootstrap the optical and X-ray images we attempted to isolate background galaxies/AGNs, but found too few to obtain reliable relative astrometry. Therefore we decided to use the obvious GC-LMXB matches themselves to recalculate the plate solution of the Chandra image and bootstrap it to the USNO system. Note that though we calculate the plate solution of the X-ray image using GC-LMXB matches, we then use the X and Y positions of the X-ray detections along with the plate solutions to calculate the "final" RAs and decs of the X-ray sources, which we then use to determine whether an X-ray source matches a GC. We determined the reliability of the X-ray plate solution by using different subsets of the optical GC positions to create the X-ray plate solution e.g. only the ground-based GC candidates in the outer regions of NGC 4472, only the HST identified GCs in the inner regions etc. and found that in each case we identified the same set of GC-LMXB matches. Thus we are confident that we have achieved 0.3" r.m.s. relative astrometric accuracy by the bootstrapping procedure identified here. This is likely to be the best optical to X-ray astrometric accuracy obtained to date.

All positions reported in the tables are in the USNO A2.0 coordinates.

3. SOURCE CATALOGS

3.1. X-ray catalogs

We detect a total of 148 sources - 136 in the full band, 11 in the soft band only, and 1 in the hard band only. Sources are considered to be matches if there is a positional offset between the different bands of less than 1 arcsecond. Three sources are within 8 arcseconds of the center of the galaxy and appear to be associated either with a weak active galactic nucleus or with brightness enhancements in the hot interstellar gas - these sources are discussed in section 7. One additional source appears to be a spurious detection, as WAVDETECT assigns it a count rate of 1.5 counts, and visual inspection fails to find evidence of a source at that location. Furthermore, the background region around this source contains more photons than the source region. This source is flagged in the table, with all its parameter values except the position listed as zeroes. The remaining 144 sources should mostly be X-ray binaries associated with NGC 4472, with about 10 likely to be foreground stars or background active galactic nuclei (see Paper I and references within).

In Table 1, we list the X-ray ID number (with the sources sorted by right ascension), IAU name, power law index, flux in the 0.5-2.0 keV, flux in the 2.0-8.0 keV band, the luminosities from 0.5-8.0 keV assuming the power law model, a distance of 16 Mpc, and isotropic emission. We include flags for the "good" sources (i.e. those which appear to be real and to be point sources upon visual inspection),

whether the source is within one or more of the HST fields of view, and the optical ID numbers of the optical counterparts where such counterparts exists.

3.2. Optical catalogs

Within the HST regions, we detect 1102 optical sources whose half light radii are small enough to be globular cluster candidates, using the source detection algorithm of Kundu & Whitmore (2001) - see also Paper I. In Table 2, we list the ID numbers (sorted by right ascension), V band magnitude, I band magnitude, $V - I$ color, and half-light radii. We also include flags which indicate whether the source is within the Chandra field of view, and whether the source has a typical globular cluster color (i.e. $0.8 < V - I < 1.4$). There are 928 globular cluster candidates in the HST fields, 829 of which are also within the Chandra fields. Four of these sources are within the central 8 arcseconds of the galaxy, so only we attempt to match only 825 with the X-ray catalog. For sources with X-ray counterparts, the X-ray ID number is listed; for sources without, an "N" appears in this column.

3.3. The matching catalog

We match sources between the X-ray and optical lists, ignoring sources within 10 arcseconds of the center of NGC 4472, where the brightness of the hot gas and the possible weak AGN activity makes the X-ray detection procedure likely to find sources which are not X-ray binaries. We find 30 X-ray sources within 0.7 arcseconds of an optical source with optical colors consistent with being globular clusters. Two additional sources show optical colors outside the globular cluster color range and are likely to be either foreground or background objects. In table 3, we list the X-ray and optical properties of the 30 globular clusters with X-ray sources - the X-ray ID number, the IAU name, the best fitting power law spectral index, the 0.5-2 keV and 2-8 keV fluxes, the luminosity, the χ^2 and number of degrees of freedom of the spectral fit, the optical catalog ID number, the position of the optical source, the V magnitude, the I magnitude, the $V - I$ color, and the half-light radius of the optical counterpart. Throughout the remainder of this paper, we will define the "globular cluster sources" to be the members of the matching catalog and the "field sources" to be only those sources which do not have an optical counterpart but are within the HST field of view. Sources outside the regions observed by HST are not included in discussions of the "field sources."

4. X-RAY SPECTRAL MODELS

As this work may be of some interest to researchers generally unfamiliar with the detailed spectral properties of accreting black holes and neutron stars, we include a very brief review of the topic. It is known that the spectral form of the X-ray binary systems in the Milky Way galaxy changes with luminosity as the sources enter different spectral states. There are two key continuum components to X-ray spectra of black hole binaries in the 0.5-8.0 keV range - a multi-temperature thermal component which dominates at the lower energy end of the spectral range, and a power law tail which dominates at the higher energy end of the range. The thermal component is generally thought to arise from a geometrically thin, optically

X-Ray/HST Matches

XID	IAU Name	Γ	F(0.5-2 keV)	F(2-8 keV)	Lum	χ^2	ν	OID	Position	V	I	V-I
18	CXOMKZ J1229402+075829	2.00(fixed)	1.77×10^{-15}	1.87×10^{-15}	1.12×10^{38}	0.0	3	4	12 29 40.2 +7 58 30.0	22.77±0.02	21.80±0.02	0.97±0.02
22	CXOMKZ J1229410+080003	2.00(fixed)	9.35×10^{-16}	9.84×10^{-16}	5.88×10^{37}	1.4	3	29	12 29 41.0 +8 0 3.7	21.88±0.02	20.61±0.02	1.26±0.02
27	CXOMKZ J1229416+080059	1.36 ± 0.76	9.18×10^{-16}	1.76×10^{-15}	8.22×10^{37}	0.4	3	68	12 29 41.6 +8 0 59.4	23.11±0.06	22.26±0.06	0.85±0.06
28	CXOMKZ J1229416+080015	0.96 ± 0.37	2.87×10^{-15}	1.26×10^{-14}	4.75×10^{38}	2.1	4	70	12 29 41.6 +8 0 14.8	22.88±0.04	21.56±0.04	1.32±0.04
30	CXOMKZ J1229416+080045	2.00(fixed)	7.93×10^{-16}	8.34×10^{-16}	4.99×10^{37}	1.3	3	75	12 29 41.6 +8 0 45.1	21.64±0.02	20.37±0.02	1.27±0.02
31	CXOMKZ J1229416+080049	2.00(fixed)	5.36×10^{-16}	5.64×10^{-16}	3.37×10^{37}	0.0	2	76	12 29 41.7 +8 0 49.8	21.99±0.02	20.96±0.02	1.03±0.02
34	CXOMKZ J1229423+080008	1.26 ± 0.15	9.56×10^{-15}	2.79×10^{-14}	1.15×10^{39}	12.9	11	137	12 29 42.4 +8 0 8.4	20.37±0.01	19.30±0.01	1.27±0.01
38	CXOMKZ J1229430+080040	2.00(fixed)	1.36×10^{-15}	1.43×10^{-15}	8.55×10^{37}	5.0	3	209	12 29 43.1 +8 0 40.2	21.11±0.01	20.10±0.01	1.01±0.02
44	CXOMKZ J1229438+080041	1.43 ± 0.48	2.01×10^{-15}	4.65×10^{-15}	2.04×10^{38}	0.5	3	274	12 29 43.8 +8 0 41.5	21.20±0.02	19.90±0.01	1.29±0.02
45	CXOMKZ J1229438+075957	2.00(fixed)	9.67×10^{-16}	1.02×10^{-15}	6.08×10^{37}	0.4	3	280	12 29 43.8 +7 59 57.3	21.12±0.01	20.02±0.01	1.11±0.02
48	CXOMKZ J1229440+075952	1.29 ± 0.38	2.41×10^{-15}	6.73×10^{-15}	2.80×10^{38}	4.2	4	299	12 29 44.0 +7 59 52.0	23.19±0.07	21.92±0.05	1.27±0.05
50	CXOMKZ J1229442+080042	2.09 ± 0.81	1.48×10^{-15}	1.39×10^{-15}	8.79×10^{37}	0.3	3	317	12 29 44.2 +8 0 42.5	20.86±0.01	19.62±0.01	1.24±0.02
52	CXOMKZ J1229450+075950	1.52 ± 0.25	4.62×10^{-15}	9.38×10^{-15}	4.29×10^{38}	1.3	6	408	12 29 45.1 +7 59 50.9	21.83±0.03	20.51±0.03	1.32±0.04
61	CXOMKZ J1229457+075743	2.00(fixed)	1.72×10^{-15}	1.81×10^{-15}	1.08×10^{38}	2.3	3	509	12 29 45.8 +7 57 44.1	21.60±0.01	20.29±0.01	1.31±0.01
64	CXOMKZ J1229461+075915	1.84 ± 0.26	6.22×10^{-15}	8.12×10^{-15}	4.40×10^{38}	3.8	8	543	12 29 46.1 +7 59 15.9	23.83±0.06	22.48±0.05	1.35±0.05
65	CXOMKZ J1229463+075949	1.12 ± 0.73	9.20×10^{-16}	3.26×10^{-15}	1.28×10^{38}	2.1	6	566	12 29 46.3 +7 59 49.3	21.38±0.01	20.24±0.01	1.14±0.02
66	CXOMKZ J1229464+080127	2.00(fixed)	9.40×10^{-16}	9.90×10^{-16}	5.92×10^{37}	2.9	3	571	12 29 46.4 +8 1 27.3	24.17±0.08	23.12±0.07	1.05±0.11
75	CXOMKZ J1229470+075847	1.73 ± 0.69	1.34×10^{-15}	2.04×10^{-15}	1.04×10^{38}	0.0	3	663	12 29 47.0 +7 58 47.4	21.79±0.01	20.55±0.01	1.24±0.01
79	CXOMKZ J1229477+075926	1.07(bad fit)	1.68×10^{-15}	6.32×10^{-15}	2.45×10^{38}	9.9	4	748	12 29 47.8 +7 59 26.3	22.63±0.03	21.36±0.03	1.26±0.04
82	CXOMKZ J1229479+075919	2.00(fixed)	1.27×10^{-15}	1.33×10^{-15}	7.97×10^{37}	0.1	3	764	12 29 47.9 +7 59 19.6	21.33±0.01	20.13±0.01	1.20±0.01
90	CXOMKZ J1229491+08 027	2.00(fixed)	7.27×10^{-16}	7.66×10^{-16}	4.58×10^{37}	5.2	3	861	12 29 49.1 +8 0 27.9	22.90±0.03	21.73±0.03	1.17±0.04
92	CXOMKZ J1229493+075753	0.97 ± 0.36	2.95×10^{-15}	1.28×10^{-14}	4.84×10^{38}	2.5	4	882	12 29 49.4 +7 57 54.0	21.00±0.01	20.00±0.01	1.00±0.01
93	CXOMKZ J1229495+075925	2.00(fixed)	9.34×10^{-16}	9.83×10^{-16}	5.88×10^{37}	0.0	3	909	12 29 49.6 +7 59 25.7	21.59±0.01	20.30±0.01	1.29±0.01
95	CXOMKZ J1229501+075944	1.89 ± 0.78	1.59×10^{-15}	1.94×10^{-15}	1.08×10^{38}	2.0	4	966	12 29 50.1 +7 59 44.2	21.41±0.01	20.28±0.01	1.13±0.01
99	CXOMKZ J1229504+080014	1.59 ± 0.53	4.79×10^{-15}	8.89×10^{-15}	4.19×10^{38}	5.1	6	985	12 29 50.4 +8 0 14.2	21.26±0.01	19.96±0.01	1.30±0.01
102	CXOMKZ J1229509+08 010	1.35 ± 0.32	4.29×10^{-15}	1.10×10^{-14}	4.70×10^{38}	3.9	5	1008	12 29 50.9 +8 0 10.4	23.61±0.04	22.45±0.05	1.16±0.05
106	CXOMKZ J1229513+075917	2.00(fixed)	9.30×10^{-16}	9.80×10^{-16}	5.86×10^{37}	1.1	3	1030	12 29 51.4 +7 59 17.7	21.75±0.01	20.57±0.01	1.18±0.01
111	CXOMKZ J1229517+075960	2.48 ± 0.84	1.27×10^{-15}	6.96×10^{-16}	6.04×10^{37}	0.0	3	1041	12 29 51.7 +8 0 0.5	20.39±0.00	19.14±0.00	1.25±0.01
113	CXOMKZ J1229525+080002	2.00(fixed)	7.67×10^{-16}	8.08×10^{-16}	4.83×10^{37}	0.9	3	1066	12 29 52.5 +8 0 2.4	23.56±0.04	22.35±0.03	1.21±0.02
121	CXOMKZ J1229533+075952	1.07 ± 0.51	1.78×10^{-15}	6.70×10^{-15}	2.60×10^{38}	1.0	4	1086	12 29 53.4 +7 59 52.4	21.99±0.01	20.98±0.01	1.01±0.02

TABLE 1

THE TABLE OF X-RAY/OPTICAL MATCHES.

thick accretion disk where the disk’s temperature varies as $R^{-3/4}$ (Shakura & Sunyaev 1973), and the power law tail is generally thought to arise from Compton upscattering of the disk photons in a cloud of hot electrons (see e.g. Sunyaev & Titarchuk 1980).

The three basic bright spectral states seen in black hole systems are, in order of increasing luminosity, the low/hard state, characterized by a $\Gamma \sim 1.5$ power law, the high/soft state, characterized by a disk blackbody component with $kT_{inner} \sim 1 - 2$ keV and a weak $\Gamma = 2.5$ power law, and the very high state, which is similar to the high/soft state, except that the power law component, rather than the disk component dominates the bolometric luminosity of the very high state. For Galactic sources, the rapid variability properties can also help in classifying the spectral state of a source, but extragalactic X-ray sources are far too faint for these techniques to be of use. For a more detailed discussion of the spectral and variability characteristics of sources in the different spectral states, we refer the readers to Nowak (1995) and Tanaka & Lewin (1995), which discuss black hole binaries, and van der Klis (1995) which includes some discussion of black hole systems but focuses more heavily on neutron star systems.

Neutron stars also show different spectral states but they are generally classified using a different nomenclature (see e.g. van der Klis 1995). The low magnetic field neutron stars have typically been broken into two classes - the atoll sources and the Z-sources, although this distinction has been blurred by recent observations (see e.g. Muno, Remillard & Chakrabarty 2002). The high-magnetic field neutron stars are predominantly accretion-powered pulsars, where the accreted matter is funneled down the magnetic poles. About 90% of X-ray pulsars in the Galaxy are found in high mass X-ray binaries, the few which are in LMXBs all emit at well below 10^{37} ergs/sec (Liu et al. 2001 and references within). The atoll sources (or “atoll-state” sources) are all also much fainter than our detection limits. Thus, all the neutron star sources detection in these observations (and most observations of elliptical galaxies made to date) are likely to be Z sources. The spectra of Z sources are rather complicated, but typically are well fit by a model dominated by thermal Comptonization is an optically thick ($\tau \sim 10$), relatively low temperature ($k_B T \sim 3$ keV) medium (see e.g. di Salvo et al. 2001).

In this paper, we will fit three spectral models to the observed data. Two of these models, the power law model and the thermal bremsstrahlung model, are standard spectral models. These two models have been fit to X-ray spectral data since the earliest days of X-ray spectroscopy because they often provide good parameterizations of the data. The power law model fits a normalization and a spectral index Γ , defined such that $\frac{dN}{dE} \propto E^{-\Gamma}$. The bremsstrahlung model is parameterized in terms of a normalization and a temperature, generally expressed in keV. The third model we fit is the disk blackbody model (Mitsuda et al. 1984), which models the spectrum of a standard accretion disk. It is parameterized in terms of a temperature at the inner edge, generally expressed in keV and a normalization. While other models, such as thermal Comptonization models, may provide a more physically motivated description of the spectra, these models typically require too many physical parameters to be fit

given the relatively small number of photons observed with Chandra.

5. THE X-RAY SPECTRAL PARAMETERS

5.1. Comparison between cluster members and non-members

While a substantial fraction of the LMXBs in NGC 4472 (and other elliptical galaxies) are clearly not associated with globular clusters, it is not yet clear that these sources were formed outside globular clusters. Stars may be ejected from globular clusters in stellar collisions, and this effect is likely to be most important for hard (i.e. tight) binary systems (see e.g. Phinney & Sigurdsson 1991). Additionally, globular clusters may be destroyed by evaporation and tidal interactions with the galactic potential, leaving behind whatever X-ray binaries they contained as field sources (see e.g. Murali & Weinberg 1997; Vesperini 2000). If the formation mechanism for the bulk of the field sources is different than the formation mechanism for the globular cluster sources, then one might expect to see a difference between the X-ray spectra of the field sources and those of the globular cluster sources. On the other hand, the luminosity functions of the field and cluster sources have already been shown to be consistent with one another (Paper I). Since the spectral properties of accreting compact objects are generally well-tied to the accretion rate in Eddington units (see the discussion in the previous subsection), one would only expect a difference in the spectral properties if the field and cluster sources if the sources below the Eddington limit for a neutron star were composed mostly of high Eddington fraction neutron stars in one case and of low Eddington fraction black holes in the other. It is not clear whether the field and cluster LMXB populations should be contain the same relative fractions of black hole and neutron star primaries. Thus it may be beneficial to test whether the spectral properties of the field and cluster sources are consistent with one another.

Given this motivation, we extract a composite X-ray spectrum for the field sources and composite spectrum for the globular cluster sources. As above, we bin the data so that at least 20 photons are included in each channel, ignore channels below 0.5 keV and above 8.0 keV, and fix the neutral hydrogen absorption column at $1.6 \times 10^{20} \text{cm}^{-2}$ (the Galactic value along the line of sight to NGC 4472). We then fit an absorbed power law model to both summed spectra. For the field sources, we find the photon index, $\Gamma = 1.44 \pm 0.10$ (90% confidence interval), while for the globular cluster sources, $\Gamma = 1.38 \pm 0.10$. A bremsstrahlung model gives $kT_{GC} = 17.5 \pm_{6.5}^{20.5}$ keV and $kT_{field} = 11.5 \pm_{4.1}^{10.3}$ keV, while a disk blackbody model (diskbb in XSPEC - see Mitsuda et al. 1984) gives $kT_{GC} = 1.53 \pm_{0.20}^{0.24}$ keV and $kT_{GC} = 1.38 \pm_{0.17}^{0.22}$ keV for the inner disk temperatures. Thus we find that the summed spectra of the globular cluster and field sources are consistent with being the same.

We note that the spectral indices and bremsstrahlung temperatures we find here indicate a somewhat harder spectrum than that typically found for the hard excess in elliptical galaxies from ASCA observations. Multiple explanations are possible. The first is that, because our detection threshold is at $\sim 10^{37}$ ergs/sec, we are biased

towards sources that have hard spectra in the 0.5-8 keV range. To those familiar with state transitions in the X-ray band, this may seem counter-intuitive, as the “hard” state for black holes typically occurs at luminosities less than $\sim 5 \times 10^{37}$ ergs/sec, so a fraction of the black holes observed should be hard state objects. However, the spectra of the high/soft state are typically dominated by a thermal disk component with a temperature of $\sim 1 - 2$ keV (i.e. similar to the observed composite spectrum). The effective area of Chandra drops above the peak of the disk blackbody, so moderate depth Chandra observations will not be particularly sensitive to this cutoff. Hence a power-law model fit, dominated by the low energy portion of the disk blackbody spectrum, is acceptable in χ^2 terms, and will tend to have a flatter spectral index than the typical low/hard state in the 0.5-8.0 keV range. Alternatively, the hard component may include a non-thermal tail to the diffuse emission (see e.g. Fujita & Sarazin 2001). Distinguishing between the two scenarios would be most effectively done with deeper X-ray observations that resolve a greater fraction of the total luminosity in X-ray sources. In order to merely verify that the sources above 5×10^{37} ergs/sec have a spectral cutoff above ~ 5 keV, XMM-Newton EPIC images could be taken, as they provide greater effective area at hard X-ray energies.

5.2. Correlation between X-ray luminosity and spectral properties

For the sources whose luminosities are higher than the Eddington limit for neutron stars, we attempt to determine if evidence for state transitions between the different black hole spectral states can be seen. Below the Eddington limit for accreting neutron stars, it will be impossible to disentangle, solely on the basis of luminosity, neutron stars accreting at a high fraction of the Eddington luminosity from black holes accreting at a lower fraction of the Eddington luminosity. We thus restrict this analysis to sources above the Eddington limit for a neutron star. The Eddington limit for a neutron star occurs at about 15% of the Eddington luminosity for a $10 M_{\odot}$ black hole. Typical luminosities for the state transition from the low/hard to the high/soft state are $\sim 5 - 10\%$ of the Eddington luminosity, while the transition from the high/soft to the very high state typically occurs at about 30% of the Eddington luminosity, although hysteresis is sometimes seen in the state transitions (see e.g. Nowak, Wilms & Dove 2002; Maccarone & Coppi 2002).

We create two groups of sources from which to make summed spectra - the sources with luminosities between 2 and 4×10^{38} ergs/second, which are assumed to be in the high/soft state and the sources with luminosities greater than 4×10^{38} , which are assumed to be in the very high state. We include sources with and without optical counterparts. For a power law model, the high state and very high state spectral indices are 1.42 ± 0.09 and 1.44 ± 0.08 respectively. For the disk blackbody, the high/soft state fits well for $kT = 1.32 \pm_{0.14}^{0.17}$ keV, while the very high state has a best fitting temperature of $1.30 \pm_{0.14}^{0.16}$ keV; however, the very high state spectrum shows a residual excess above 4 keV and has $\chi^2/\nu = 95.8/66$, ruling out the model at the 99% confidence level. The summed “high/soft state” and “very high state” spectra are plotted in Figure 2.

This result is not particularly robust, since when we restrict the summed spectra to those with globular cluster counterparts, both the high/soft state and the very high state spectra fit well to a single disk blackbody model with temperatures consistent with being equal. Thus it is possible that one or more of the high flux sources without an optical counterpart is a background active galaxy with a hard spectrum and not a very high state black hole system in NGC 4472. This issue merits further attention in larger samples of sources. The bulk of the sources should be sufficiently well separated for XMM to observe them; XMM spectra could help determine whether there are stronger power law tails in the systems above 4×10^{38} ergs/second, since its energy coverage between 8 and 15 keV will provide good measurements in a region of the spectrum that should be dominated by the power law tail.

5.3. Comparison between red and blue cluster X-ray sources

Given that there is a clear difference between the formation efficiency of X-ray binaries in the red globular clusters and that in the blue globular clusters (Paper I), it is possible that there is a fundamental difference between the X-ray properties of the sources in the red globular clusters and those in the blue globular clusters. We thus extract summed spectra for the red and blue globular clusters separately and fit them using the same procedures as we used to compare the globular cluster and field sources.

We find that the blue globular clusters clearly have harder spectra than the red ones. The best fit power law indices of the blue and red systems are 1.02 ± 0.27 and $1.46 \pm_{0.10}^{0.11}$ respectively, while the best fitting disk blackbody inner temperatures are $2.8 \pm_{1.1}^{6.6}$ keV and $1.37 \pm_{0.18}^{0.21}$ keV, respectively. For a bremsstrahlung model, the red globular clusters are best fit by a temperature of $10.7 \pm_{3.7}^{8.7}$ keV, while the lower limit for the bremsstrahlung temperature of the blue clusters’ summed spectrum is 28 keV. The red clusters X-ray sources dominate the globular cluster system’s X-ray source population, so it is not surprising that the summed spectral properties of the red clusters are consistent with the globular cluster sample as a whole and very similar to those of the field sources. The difference between the red and blue clusters’ integrated X-ray spectra are illustrated in Figure 1.

While there is a statistically significant difference between the X-ray spectral properties of the red and blue globular cluster X-ray sources, we believe it is premature to ascribe this difference to the metallicity. There are only 7 X-ray sources in the blue globular cluster systems, and the two brightest of these systems contribute about 70% of the total luminosity in the blue globular cluster X-ray source sample. The luminosity distribution of the 23 red globular cluster X-ray sources appears less top heavy, but the two luminosity functions cannot be distinguished with a KS test. Because there are so few X-ray sources in the blue globular cluster systems, a degree of caution must be exercised in making broad statements about their nature. We thus believe only that it will be important to perform similar analyses on the globular cluster systems of other galaxies in order to determine whether the source spectra depend upon the globular cluster’s color. Some credence to the notion that this result is physically significant comes

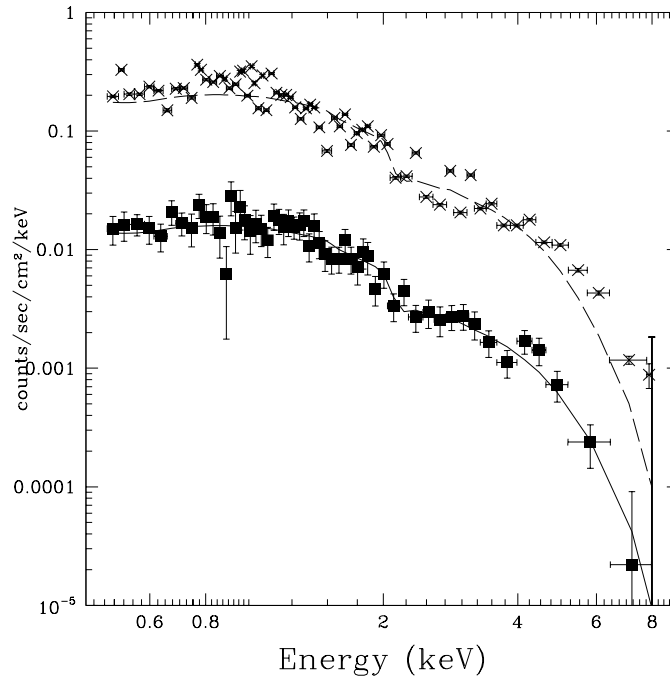


FIG. 1.— The “high/soft state” integrated spectrum (filled squares) and the “very high state” integrated spectrum (X’s). The very high state spectrum has been shifted up in normalization by a factor of 10 to make the figure less confusing. The model curves are the best fitting disk blackbody spectra. We note the systematic positive residuals in the “very high state” spectrum presents tentative evidence for a hard tail in the highest luminosity systems, much like their Galactic counterparts.

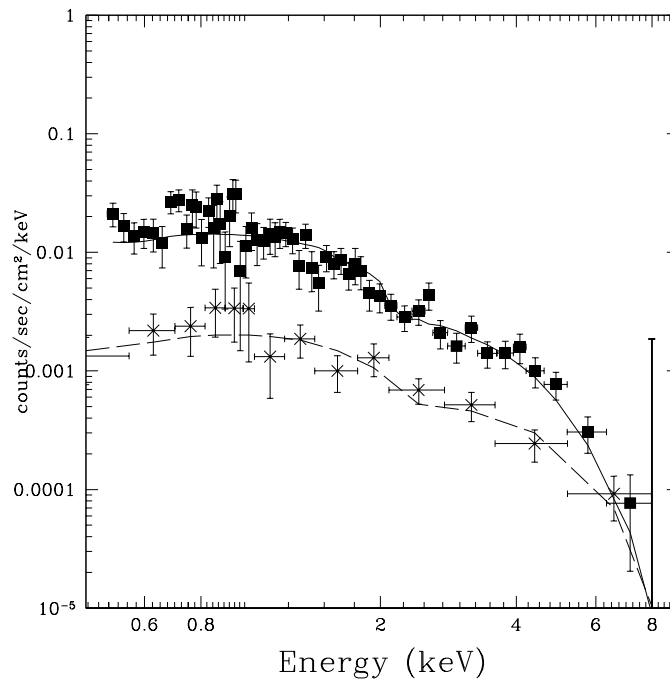


FIG. 2.— The summed spectrum of the red globular clusters (filled squares) and the blue globular clusters (X’s), along with the best fitting absorbed disk blackbody model. The red clusters’ low mean disk temperature can be seen by its steeper cutoff at high energies.

from the result of Irwin & Bregman (1999) that showed the most metal rich globular clusters in the local group had the softest spectra in the soft X-ray band observed by ROSAT.

6. HOW ARE THE LMXBS FORMED?

A key result of this investigation and of Paper I is that the properties of globular cluster LMXBs are generally consistent with those of the field LMXBs. There are several mechanisms for creating a population LMXBs which can be found in the field population rather than in the globular clusters of elliptical galaxies - (1) the presence of a large, low duty cycle transient population (Piro & Bildsten 2001), (2) ejection of binaries formed in globular clusters (e.g. Phinney & Sigurdsson 1991), and (3) tidal disruption of globular clusters, releasing systems formed in clusters into the field (see e.g. Fall & Zhang 2001; Vesperini 2000; Ostriker & Gnedin 1997). We will discuss how the observational results found here may help to determine the relative importance of the different scenarios. As we discuss the “dominant” formation mechanism here, we refer to the mechanism for forming the *observed* sources; given a sufficiently low duty cycle, there could exist many more quiescent LMXBs than LMXBs in outburst, and those sources could constitute the bulk of the LMXB population of a galaxy while at the same time contributing a small fraction of the observed sources.

6.1. *Spatial distributions and evidence for an ejection model*

The spatial distribution of the field and globular cluster LMXBs are consistent with one another and with the optical globular cluster distribution, but appear to be different from the galaxy’s field light profile (see Figure 4 of Paper I). In fact, the globular clusters show a shallower surface density than the integrated light not only in NGC 4472, but in most elliptical galaxies (see e.g. Ashman & Zepf 1998). The similarity between the LMXB and GC spatial distributions (and the differences of these from the stellar light profile) in NGC 4472 suggest that the bulk of the observed LMXBs are formed in globular clusters. If this result is confirmed in observations of additional galaxies, it would indicate that mechanism (1) above is relatively less important than mechanisms (2) and (3). If mechanism (3) were the most important, then one would expect the field LMXB distribution to be more centrally concentrated than the current observed cluster distribution, as tidal destruction of clusters is most effective in the center of the galaxy where the tidal forces are strongest (Vesperini et al. 2002, in prep.). Mechanism (2) predicts that the field LMXBs should have a slightly more spatially extended distribution than the globular cluster distribution as a whole, as the escape velocity from a globular cluster is about 10 km/sec and the lifetime of a bright persistent LMXB is about 300 million years or less, so the system will travel about 5 kiloparsecs, or about 1 arcminute from its initial location at the distance of NGC 4472. This distance will be large enough to make the initial globular cluster associated with the LMXB impossible to determine (except in the outer regions of the galaxy), but small enough that there will not be a large population of LMXBs which have traveled very far from the center of the galaxy.

The similar spectral properties of the field and cluster sources provide additional evidence that the two populations have a common origin. At the present time, no work has been done to show whether the long timescale transients should spend the same fraction of their lives in the different spectral states as do the shorter period transients and persistent sources, but it would seem to be an unusual coincidence if they did. The identical luminosity functions and summed spectra of the two populations present a challenge to any mechanism which posits a different origin for the cluster sources than for the bulk of the field sources. As noted above, the luminosity functions present a stronger constraint on these grounds than do the spectral properties. Spectral properties are generally well-tied to a source’s fraction of the Eddington luminosity, so given identical luminosity functions and identical proportions of black holes and neutron stars, one would expect *a priori* identical summed spectral properties. The proportion of black holes and neutron stars among the sources above 10^{37} ergs/sec may differ for transient and persistent source, but this is presently not clear. Hence, at the present, the identical luminosity functions present stronger evidence for the common origin of the bulk of the field and globular cluster sources.

It should be noted that mechanisms (1) and (3) may be at play in addition to mechanism (2). In fact, transient systems have been seen in the field LMXB populations of elliptical galaxies (Kraft et al. 2001), although it will not be clear without multi-epoch observations of some elliptical galaxies what fraction of these transients have long recurrence timescales and hence low duty cycles. Some or all of them may be like the Galactic source Aql X-1, which is a transient, but has a recurrence timescale of roughly one year and a duty cycle of about 20%. Additionally, low duty cycle transients may be present within the globular clusters as well as the field sources.

There are several reasons why, if ejections supply a substantial fraction of the field sources, then these ejections are likely to be caused by collisions and not by supernova kicks. Firstly, binaries immediately ejected by supernova kicks take no advantage of the stellar interaction rates in the globular clusters - they should be formed at the same rate in globular clusters as in the field, which means that they should account for $\lesssim 0.1\%$ of the field X-ray binaries in their host galaxies. Secondly, the binaries most likely to be long period, low duty cycle transients when their secondary stars evolve off the main sequence (Piro & Bildsten 2001) are also more likely to have small velocity kicks (Brandt & Podsiadlowski 1995; BP95). Thirdly, it has been suggested that black hole systems tend to have systematically lower velocity kicks than neutron stars (BP95), which means that if the ejected systems leave immediately after becoming the supernova explosions, then the globular cluster systems would be expected to have a substantially larger black hole fraction than the field, while the observations show no signature of this effect.

6.2. *Implications of the GC color-spectral index correlation*

If the correlation between globular cluster color and spectral index of the X-ray sources is verified, possible causes might be a dependence on metallicity of the rel-

ative proportion of black hole and neutron star primaries in the X-ray binaries or of the mean binary separation and hence mean accretion rate that causes different fractions of the systems to be in different spectral states depending on the metallicity. It may be, for example, that the dependence of binary fraction on globular cluster color is partly due to the fact that the red globular clusters are younger than the blue ones, rather than due to the fact that they are more metal rich, and that X-ray binaries are preferentially formed early in the lifetimes of globular clusters. If the primary formation mechanism is the hardening of existing binary systems by stellar interactions so that they can undergo Roche lobe overflow, rather than the formation of new compact object binary systems by tidal captures, then the depletion of a “reservoir” of binary systems may cause the younger (red) clusters to have more X-ray emitting systems than the older (blue) clusters. If this scenario is correct, then one would expect the blue globular cluster X-ray binary sample to have a larger fraction of transient sources, which would in turn possibly have different spectral characteristics than the steady accretors. At the present, no definitive statement can be made on this topic. Our future work will include observations of systems such as NGC 4365, NGC 3115 and NGC 1399 where there is broader band optical data which can be used to place stronger constraints on the red globular clusters’ ages, and theoretical investigations to determine whether the “reservoir depletion” scenario outlined above is capable of quantitatively reproducing the observations. Additionally, multiple epoch observations with Chandra can help determine whether the blue cluster sources are more likely than the red cluster sources to be transient systems and whether the field or globular clusters sources are more likely to be transients. At present, only one elliptical galaxy in which the X-ray point source population can be well studied, NGC 5128, has been observed twice and it was found that a substantial fraction of its sources were transients (Kraft et al. 2001).

6.3. Comparisons with other galaxies and possible evidence for an *in situ* population

Through preliminary work we have done on the S0 galaxy NGC 3115 and the elliptical galaxy NGC 4365, we have found that roughly 25% and 35%, respectively, of the X-ray binaries in these systems are associated with globular clusters (the details of this work will appear in a future paper). This would seem to suggest that the fraction of X-ray binaries in globular clusters varies with Hubble type, with the highest fraction of globular cluster sources in the earliest type galaxies. There may additionally be some evidence for a correlation between the fraction of X-ray binaries in globular clusters and the fraction of total stellar mass in globular clusters, as NGC 1399 has the highest values in the currently well-studied sample for both these quantities and NGC 3115, the Milky Way and M31 have lower values for both these quantities (although recent star formation could explain the large number of field LMXBs in the Milky Way and M31). NGC 4472 and NGC 4365 have intermediate values for both quantities.

This correlation, if verified, would probably imply that a significant fraction of the field sources are, in fact, generated in the field. There would then be three populations

of X-ray binaries - (a) the globular cluster sources (b) the sources generated in globular clusters but released into the field and (c) the population of field X-ray binaries generated *in situ*. Let us define the number of globular cluster sources to be N_{GC} , the number of field sources created in globular clusters to be N_{FGC} , and the number of field sources produced *in situ* to be N_{IS} . Furthermore, let us define the ratio between the number of globular cluster X-ray sources and the number of field sources produced in globular clusters to be η , so that $N_{FGC} = \eta N_{GC}$. We then find that:

$$\frac{N_{GC}}{N_{LMXB}} = \frac{N_{GC}}{N_{GC}(1 + \eta) + N_{IS}}, \quad (1)$$

where N_{LMXB} is the total number of LMXBs in the galaxy. Thus the fraction of sources in globular clusters may depend upon η , $\frac{N_{GC}}{N_{IS}}$, or both. It might be expected, for example, that in the lenticular galaxy NGC 3115, which has the lowest estimated value of $\frac{N_{GC}}{N_{LMXB}}$ among the early-type galaxies, that η could be especially large because more stellar interactions within the globular clusters are caused by the greater tidal forces in the disk-like galaxy. Studies of a much larger sample of galaxies are needed to separate the effects of η and $\frac{N_{GC}}{N_{IS}}$.

We also find in NGC 4365 and NGC 3115 that the fraction of globular clusters with LMXBs is about 4%. This fraction is also 4% in NGC 4472 (Paper I) and NGC 1399 (Angelini, Loewenstein & Mushotzky 2001), and is 2-3% in M31 (di Stefano et al. 2002; Barmby & Huchra 2001) and 1-4% (Liu, van Paradijs & van den Heuvel 2001; Harris 1996) in the Milky Way with the large uncertainties coming from the difficulty in counting the known transients. Thus while this quantity may have some effects on the relative fractions of LMXBs in globular clusters in the spiral galaxies compared to the elliptical galaxies, it seems to be fairly universal in the ellipticals and not to be a major factor causing the wide range in the fraction of LMXBs in the field versus the fraction in globular clusters.

6.4. Discussion of selection effects

There are a few causes for concern in applying the observational constraints directly to the theoretical models. There are significant selection effects in the X-rays that make our detected sample incomplete. The X-ray completeness may vary with radial distance from the center of the galaxy due to both the degradation of the Chandra point spread function as one moves off-axis and the variation of the effective background from the diffuse gas as a function of radius. Preliminary results seem to suggest that the two effects balance one another for NGC 4472 (Kim & Fabbiano 2002). There will also be similar selection effects in the optical (the faintest clusters will be missed in the central regions of the galaxy because of the contamination from the field starlight). These should not be too severe as it is likely that there are very few X-ray sources in the faint globular clusters below the sensitivity limit of the HST observations (see Paper I). We *can* be fairly confident that the spatial distribution and the luminosity function for the field and cluster X-ray sources are consistent with one another, since the selection effects should apply to the two X-ray populations equally. The results of Kim & Fabbiano (2002) suggest that spatial pro-

file of the X-ray sources is also unaffected by selection effects, so the similarity between the spatial profiles of the optical globular cluster sample and the X-ray sources is also likely to be a real effect. The final potential problem with gleaning results from these data is that there are still relatively few sources. With only 30 sources in globular clusters, and only 11 of those at luminosities higher than the Eddington luminosity for a neutron star, comparisons of luminosity functions, for example, are likely to suffer from small number statistics.

7. VERY MASSIVE BLACK HOLES

It has been recently noted that there may be relatively large populations of very massive black holes (VMBHs) produced by supernova explosions of population III stars (Schneider et al. 2002) since the inefficiency of cooling of metal-free gas results in a top-heavy initial mass function (Abel et al. 2000; Bromm et al. 2001), and the supernova explosions of these heavy stars will result in black holes that contain a very large fraction of the initial mass being locked up in the final black hole (see e.g. Heger & Woosley 2001). It has further been suggested that Bondi-Hoyle accretion from the interstellar medium by the VMBHs could explain the bright non-nuclear X-ray source population (Schneider et al. 2002). On purely observational grounds, we cannot rule out the hypothesis that isolated accreting VMBHs represent some fraction of the X-ray sources, but we note that our finding that 40% of the X-ray sources are associated with globular clusters indicates that the observations of these sources cannot be used as a lower limit for the number of VMBHs, and that subsequent lower limits on the redshift of star formation and on the fraction of Population III stars that contribute to the metal enrichment of the early universe (Schneider et al. 2002) must be revised. The similarities of all the X-ray properties of the globular cluster and field X-ray sources would further suggest that VMBHs represent a small fraction of the field sources.

Theoretical arguments also indicate that VMBHs are unlikely to make up any of the observed X-ray sources in NGC 4472 and other elliptical galaxies. For NGC 4472 (and in fact, for most elliptical galaxies), the Bondi-Hoyle accretion rate (Bondi 1952) is far too low to supply a $200 M_{\odot}$ black hole with enough mass to be observable at the detection threshold of $\sim 10^{37}$ ergs/sec. The Bondi-Hoyle accretion rates of the $\sim 10^9 M_{\odot}$ black holes at the centers of elliptical galaxies are typically of order $1 M_{\odot}/\text{yr}$ (di Matteo et al. 2000), and given that the Bondi-Hoyle rate scales with M^2 of the accreting object, the accretion rate for a $\sim 200 M_{\odot}$ black hole should be $\sim 10^{-14} M_{\odot}/\text{yr}$, or 7×10^{11} g/sec, which would provide a luminosity of 6×10^{31} ergs/sec given the standard $0.1c^2$ efficiency, or a substantially lower luminosity given the reduced radiative efficiencies expected to be seen at very low accretion rate (see e.g. Rees et al. 1982; Narayan & Yi 1994; Blandford & Begelman 1999; di Matteo et al. 2000; Quataert & Gruzinov 2000). Because the Bondi-Hoyle accretion rate also goes as $T^{-3/2}$, the neutral interstellar medium may actually contribute more mass than the hot X-ray emitting gas; for NGC 4472 (as in most elliptical galaxies), the upper limit on the neutral hydrogen gas mass is a factor of ~ 200 lower than the mass of the X-ray emitting gas

(Kumar & Thonnard 1983). We can thus place a limit on the Bondi-Hoyle accretion rate of the neutral hydrogen at 1×10^{14} g/sec and hence on the luminosity of 1×10^{34} , so we still would not expect to observe such sources. Accretion onto isolated VMBHs thus may be of some importance in spiral galaxies, where the interstellar medium may be colder and denser (in molecular clouds, for example), and hence the Bondi-Hoyle accretion rate may be higher, but cannot explain X-ray sources in any low redshift elliptical galaxies except the ones most rich in neutral hydrogen. As VMBHs should be undetectable in NGC 4472, they may still contribute to the dark matter budget as suggested by Schneider et al. (2001).

8. THE NUCLEAR EMISSION

Three point sources are detected within $8''$ of the nucleus. The brightest, source 71 in the X-ray list, is likely to be a very weak active galactic nucleus, with a luminosity of about 10^{39} ergs/second. Previous studies of these same data for NGC 4472 failed to identify this source as a point source (Loewenstein et al. 2001), most likely because these analyses used the CELLDetect algorithm to identify point sources rather than the more sensitive WAVDETECT algorithm used in our work. The 0.5-8 keV luminosity of our detected source is very close to the 2-10 keV upper limit determined by Loewenstein et al. (2001), so conclusions about the radiative efficiency of this source are not significantly changed. Observations of weak radio lobes in NGC 4472 indicate a minimum energy content of only 10^{54} ergs with a corresponding equipartition magnetic field of 10^{-9} G, which gives a minimum particle lifetime of $\sim 10^8$ years, and hence requires a minimum luminosity of only $\sim 3 \times 10^{38}$ ergs/sec. Hence, it is not surprising to find that the X-ray luminosity of the NGC 4472 nucleus is so low. We find the position of the optical center to be $\alpha = 12 : 29 : 46.78$, $\delta = 8 : 00 : 02.2$ in the USNO system, about $1''$ arcsecond from the X-ray center, and within the rounding errors of the radio core position (Ekers & Kotanyi 1978). We find an offset of about $2''$ with regards to the SIMBAD optical center position, but our optical center should be far more reliable and we find good agreement with the position of the center reported by NED.

The two other point sources are collinear with the presumed nucleus and the major axes of their source ellipses as detected by WAVDETECT are approximately parallel to the line connecting the sources. Furthermore, the line connecting the sources is perpendicular to the weak core-dominated radio jets seen in previous observations (Ekers & Kotanyi 1978). Recently, equatorial radio emission has been seen simultaneously with jet emission in the Galactic source SS 433 (Paragi et al. 1998,1999a,1999b; Blundell et al. 2001), and it has been suggested that at least a fraction of the X-ray emission seen from this source might come from the equatorial outflow if the equatorial radio emission is produced by bremsstrahlung processes (Blundell et al. 2001). Strong disk winds are predicted at very high accretion rates (in sources such as the likely super-Eddington SS 433) or low accretion rates in sources such as NGC 4472 by theoretical work (see e.g. Blandford & Begelman 1999), and may be responsible for the production of such ‘‘ruffs’’ and the very low radiative efficiency of the AGN in NGC 4472. The radio observations initially

used to detect the jet in NGC 4472 had very poor North-South angular resolution and would not have been capable of resolving a ruff in this source. Deep, high resolution radio images are needed to test whether the equatorial X-ray sources are associated with a disk wind or the alignment of the sources on an axis perpendicular to the radio jet is a coincidence.

9. CONCLUSIONS

Source lists for the optical and X-ray sources in NGC 4472 are presented. The X-ray properties of the sources associated with globular clusters are consistent with those of the sources without optical counterparts. The mean X-ray spectrum of the sources in the blue globular clusters is harder than that in the red globular clusters but this result may be spurious because there are so few X-ray sources in the blue globular clusters. There is marginal evidence for a hard tail in the sources whose luminosities indicate they are in the very high state, and no evidence for such a tail in the sources whose luminosities indicate they are in the soft state. We show that the current observational evidence suggests tentatively that the bulk of the field sources were ejected from globular clusters. On the other hand, a tentative correlation between the fraction of LMXBs in globular clusters and the fraction of stellar mass

in globular clusters across the four well-studied elliptical galaxies suggests that there may also be a field population generated *in situ*. We discuss future observations which may help test this picture. We show that accreting isolated very massive black holes cannot produce observable X-ray sources in NGC 4472 or most other elliptical galaxies. There is possible evidence for an equatorial “ruff” near the galactic nucleus which may be associated with a disk wind.

10. ACKNOWLEDGMENTS

We gratefully thank Kathy Rhode for providing us with her large field of view optical image which was essential for this study to tie together accurately the various HST images to the Chandra image and all the satellite images to the USNO system. We thank Lars Bildsten for a critical review of this manuscript. This research has made use of the NASA/IPAC Extragalactic Database (NED) which is operated by the Jet Propulsion Laboratory, California Institute of Technology, under contract with the National Aeronautics and Space Administration. This research has made use of the SIMBAD database, operated at CDS, Strasbourg, France. SEZ and AK gratefully acknowledge support from NASA via the LTSA grant NAG5-11319.

REFERENCES

- Abel, T., Bryan, G. & Norman, M., 2000, *ApJ*, 540, 39
 Angelini, L., Loewenstein, M. & Mushotzky, R.F., 2001, *ApJL*, 557, 35
 Arnaud, K.A., 1996, *ASp Conf. Ser.*, 107, 17 (eds. G. Jacoby & J. Barnes)
 Ashman, K.M. & Zepf, S.E., 1998, *Globular Cluster Systems*, Cambridge University Press:Cambridge
 Baganoff, F. 1999, *ACIS On-Orbit Background Rates and Spectra from Chandra OAC Phase 1 (ACIS Memo. 162)* (Cambridge: Cent. Space Res.)
 Barmby, P. & Huchra, J.P., 2001, *AJ*, 122, 2458
 Bhattacharya, D., 1995, in *X-Ray Binaries*, eds. Lewin, van Paradijs, and van den Heuvel, Cambridge University Press:Cambridge
 Blandford, R.D. & Begelman, M.C., 1999, *MNRAS*, 303, 1L
 Blundell, K.M., Mioduszewski, A.J., Muxlow, T.W.B., Podsiadlowski, P. & Rupen, M.P., 2001, *ApJL*, 562, 79
 Bondi, H., 1952, *MNRAS*, 112, 195
 Brandt, N. & Podsiadlowski, P., 1995, *MNRAS*, 274, 461
 Bromm, V., Ferrara, A., Coppi, P.S. & Larson, R.B., 2001, *MNRAS*, 328, 969
 Dickey, J.M. & Lockman, F.J., 1990, *ARA&A*, 28, 215
 di Matteo, T., Quataert, E., Allen, S.W., Narayan, R. & Fabian, A.C., 2000, *MNRAS*, 311, 507
 di Salvo, T., Robba, N.R., Iaria, R., Stella, L., Burderi, L., Isarel, G.L., 2001, *ApJ*, 554, 49
 di Stefano, R., Kong, A.K.H., Garcia, M.T., Barmby, P., Greiner, J., Murray, S.S., & Primini, F.A., 2002, *ApJ*, 570, 618
 Ekers, R.D. & Kotanyi, C.G., 1978, *A&A*, 67, 47
 Fall, S.M. & Zhang, Q., 2001, *ApJ*, 561, 751
 Forman, W., Jones, C. & Tucker, W., 1985, *ApJ*, 293, 102
 Fujita, Y. & Sarazin, C.L., 2001, *ApJ*, 563, 660
 Harris, W.E., 1996, *AJ*, 112, 1487
 Heger, A. & Woosley, S.E., 2001, *ApJ*, 567, 532
 Irwin, J.A. & Bregman, J.N., 1999, *ApJL*, 510, 21
 Kim, D.-W. & Fabbiano, G., 2002, *APS*, 17.098
 Kraft, R.P., Kregenow, J.M., Forman, W.R., Jones, C. & Murray, S.S., 2001, *ApJ*, 560, 675
 Kumar, C.K. & Thonnard, N., 1983, *AJ*, 88, 260
 Kundu, A., Maccarone, T.J. & Zepf, S.E., 2002, *ApJL*, 574, 5
 Kundu, A. & Whitmore, B.C., 2001, *AJ*, 121, 2950
 Liu, Q.Z., van Paradijs, J. & van den Heuvel, E.P.J., 2001, *A&A*, 368, 1021
 Loewenstein, M., Mushotzky, R.F., Angelini, L., Arnaud, K.A. & Quataert, E., 2001, *ApJL*, 555, 21
 Maccarone, T.J. & Coppi, P.S., 2002, *MNRAS*, in press (astro-ph/0209116)
 Macri, L.M., et al., 1999, *ApJ*, 521, 155
 Mitsuda, K., Inoue, H., Koyama, K., Makishima, K., Matsuoka, M., Ogawara, Y., Suzuki, K., Tanaka, Y., Shibazaki, M. & Hirano, T., 1984, *PASJ*, 36, 741
 Monet, D., 1998, *PMM USNO-A2.0 Catalog*
 Muno, M.P., Remillard, R.A. & Chakrabarty, D., 2002, *ApJL*, 568, 35
 Murali, C. & Weinberg, M.D., 1997, *MNRAS*, 288, 767
 Narayan, R. & Yi, I. 1994, *ApJL*, 428, 13
 Nowak, M.A., Wilms, J. & Dove, J.B., 2002, *MNRAS*, 332, 856
 Nowak, M.A., 1995, *PASP*, 107, 1207
 Ostriker, J.P. & Gnedin, O.Y., 1997, *ApJ*, 487, 667
 Paragi, Z., Vermeulen, R.C., Fejes, I., Schilizzi, R.T., Spencer, R.E. & Stirling, A.M., 1998, *NewA Rev.*, 42, 641
 Paragi, Z., Vermeulen, R.C., Fejes, I., Schilizzi, R.T., Spencer, R.E. & Stirling, A.M., 1999a, *A&A*, 348, 910
 Paragi, Z., Vermeulen, R.C., Fejes, I., Schilizzi, R.T., Spencer, R.E. & Stirling, A.M., 1999b, *NewA Rev.*, 42, 553
 Piro, A.L. & Bildsten, L., 2002, *ApJL*, 571, 103
 Phinney, E.S. & Sigurdsson, S., 1991, *Nature*, 349, 220
 Quataert, E. & Gruzinov, A., 2000 *ApJ*, 539, 809
 Rees, M.J., Phinney, E.S., Begelman, M.C. & Blandford, R.D., 1982, *Nature*, 295, 17
 Rhode, K.L. & Zepf, S.E., 2001, *AJ*, 121, 210
 Sarazin, C.L., Irwin, J.A. & Bregman, J.N., 2001, *ApJ*, 556, 533
 Schneider, R., Ferrara, A., Natarajan, P. & Omukai, K., 2002, *ApJ*, 571, 30
 Shakura, N.I. & Sunyaev, R.A., 1973, *A&A*, 24, 337
 Sunyaev, R.A. & Titarchuk, L.G., 1980, *A&A*, 86, 121
 Tanaka, Y. & Lewin, W.H.G., 1995, in *X-Ray Binaries*, eds. Lewin, van Paradijs, and van den Heuvel, Cambridge University Press:Cambridge
 Trinchieri, G. & Fabbiano, G., 1985, *ApJ*, 296, 447
 van der Klis, M., 1995, in *X-Ray Binaries*, eds. Lewin, van Paradijs, and van den Heuvel, Cambridge University Press:Cambridge
 Vesperini, E., 2000, *MNRAS*, 318, 841
 White, R.E., Sarazin, C.L. & Kulkarni, S.R., 2002, *ApJL*, 571, 23

TABLE 2
THE X-RAY SOURCE LIST

ID	IAU Name	Γ	$\sigma_{\Gamma+}$	$\sigma_{\Gamma-}$	$F_x(.5-2)$	$F_x(2-8)$	L_x	χ^2	ν	GR	HST	OID
1	CXOMKZ J1229314+080055	2.00			8.07E-16	8.50E-16	5.08E+37	0.0	3	Y	N	
2	CXOMKZ J1229331+080218	1.66	0.44	0.41	2.69E-15	4.53E-15	2.22E+38	3.6	4	Y	N	
3	CXOMKZ J1229345+080032	1.18	0.17	0.16	7.05E-15	2.27E-14	9.13E+38	14.9	8	Y	N	
4	CXOMKZ J1229350+080049	1.20	0.45	0.37	1.83E-15	5.78E-15	2.33E+38	2.8	3	Y	N	
5	CXOMKZ J1229359+080054	2.00			6.56E-16	6.91E-16	4.13E+37	0.0	2	Y	N	
6	CXOMKZ J1229368+080311	1.02	0.56	0.49	2.15E-15	8.65E-15	3.31E+38	0.3	3	Y	N	
7	CXOMKZ J1229369+080311	1.09	0.55	0.47	2.17E-15	7.96E-15	3.10E+38	0.0	3	Y	N	
8	CXOMKZ J1229378+080046	2.00			6.53E-16	6.88E-16	4.11E+37	0.0	2	Y	N	
9	CXOMKZ J1229378+075846	1.28	0.56	0.51	4.76E-15	1.35E-14	5.59E+38	0.2	3	Y	N	
10	CXOMKZ J1229381+075838	2.00			2.28E-15	2.40E-15	1.44E+38	0.0	2	Y	N	
11	CXOMKZ J1229382+080235	2.00			1.60E-15	1.69E-15	1.01E+38	0.0	3	Y	N	
12	CXOMKZ J1229382+080013	2.00			5.87E-16	6.19E-16	3.70E+37	0.0	2	Y	N	
13	CXOMKZ J1229383+080030	1.20	0.54	0.51	2.01E-15	6.37E-15	2.57E+38	0.2	3	Y	N	
14	CXOMKZ J1229392+075920	2.00			1.33E-15	1.40E-15	8.38E+37	1.2	3	Y	N	
15	CXOMKZ J1229401+075927	1.47	0.33	0.29	3.45E-15	7.48E-15	3.35E+38	0.3	4	Y	N	
16	CXOMKZ J1229401+075944	2.00			5.34E-16	5.62E-16	3.36E+37	0.0	2	Y	N	
17	CXOMKZ J1229402+075944	2.00			1.18E-15	1.25E-15	7.45E+37	0.6	3	Y	N	
18	CXOMKZ J1229402+075829	2.00			1.77E-15	1.87E-15	1.12E+38	0.0	3	Y	Y	4
19	CXOMKZ J1229403+080241	2.00			3.22E-16	3.39E-16	2.02E+37	0.0	2	Y	N	
20	CXOMKZ J1229404+080225	2.00			9.27E-16	9.76E-16	5.83E+37	0.0	3	Y	N	

Note. — The complete version of this table is in the electronic edition of the Journal. The printed edition contains only a sample. The units are ergs/sec/cm² for the fluxes and ergs/sec for the luminosities. The “good region” is the region outside the central 8 arcseconds. Numbers in the OID column refer to the sources’ optical counterparts’ ID numbers in Table 3.

TABLE 3
THE OPTICAL SOURCE LIST

ID	RA	Dec	V	σ_V	I	σ_I	$V-I$	σ_{V-I}	R_{HL}	σ_R	CFOV	GC	XID
1	12 29 40.0	+8 3	29.8	22.13	0.01	21.07	0.01	1.07	0.01	0.0	1.5	Y	Y
2	12 29 40.2	+7 58	1.5	23.16	0.02	21.85	0.01	1.31	0.03	0.9	1.5	N	Y
3	12 29 40.2	+7 57	59.9	25.75	0.17	24.51	0.13	1.24	0.22	12.8	1.2	N	Y
4	12 29 40.2	+7 58	30.0	22.77	0.02	21.80	0.02	0.97	0.02	2.4	0.9	Y	Y 18
5	12 29 40.4	+7 57	55.0	23.57	0.03	22.71	0.03	0.86	0.04	1.4	0.6	N	Y

Note. — The complete version of this table is in the electronic edition of the Journal. The printed edition contains only a sample. The half-light radii are measured in arcseconds, a “Y” in the CFOV column indicates that a source is in the Chandra field of view, a “Y” in the GC column indicates a source is a good globular cluster candidate and a number in the XID column refers to the X-ray counterpart’s ID number in Table 2.